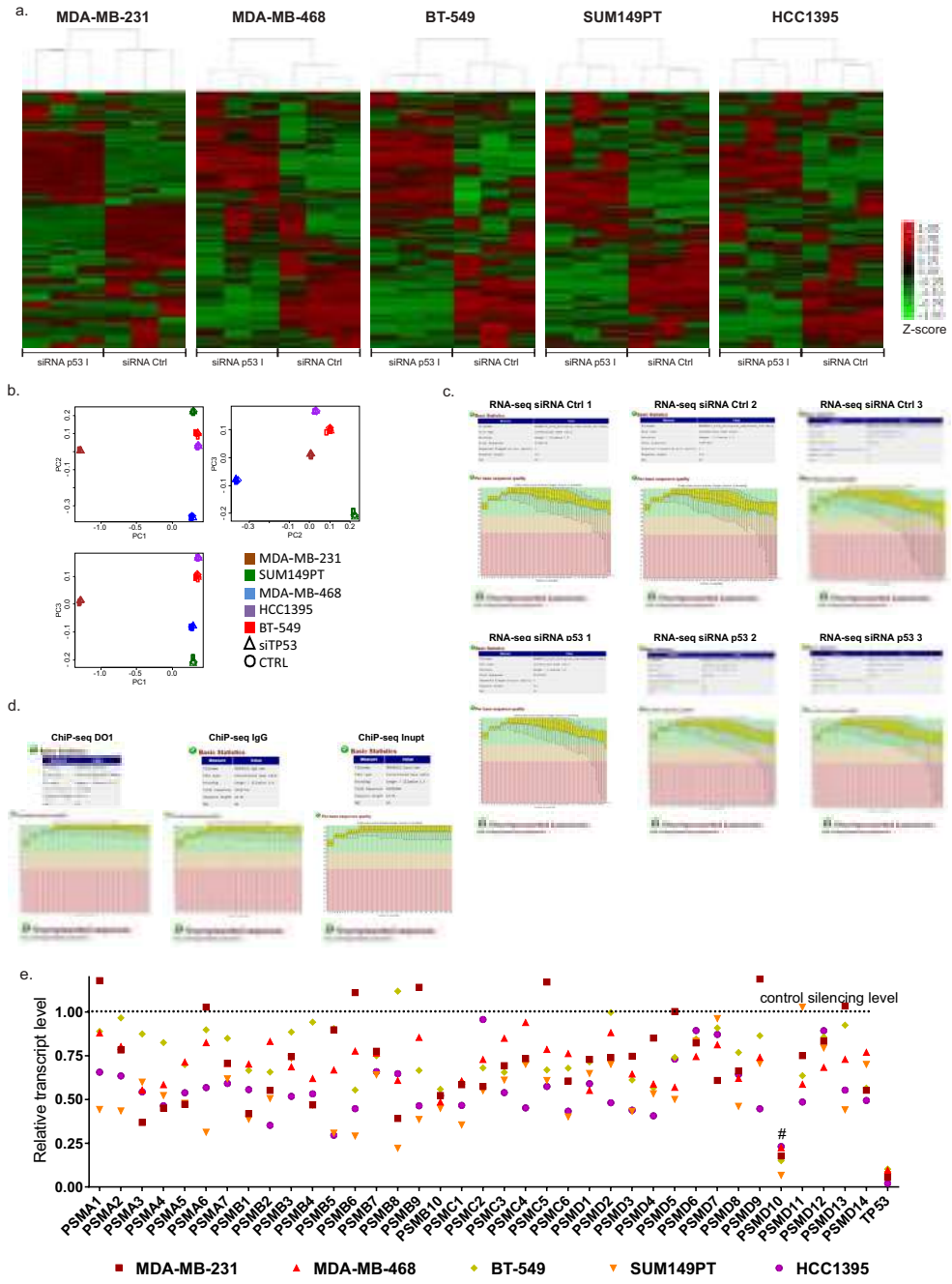

Supplementary Figure 1 a. Hierarchical clustering of gene expression data for each of the TNBC cell lines shown in Fig. 1b. In each expression matrix, after Z-score standardization, the genes with low standard deviation were filtered (MDA-MB-231: Genes 16804 (sd filter =0.05), MDA-MB-468: Genes 11428 (sd filter =0.1), BT-549: Genes 17531 (sd filter =0.1), SUM149PT: Genes 14125 (sd filter =0.1), HCC1395: Genes 10432 (sd filter =0.1)). Increased (red) or decreased (green) expression of the genes is shown for each sample. Bars below the graphs identify the samples subjected to Control (Ctrl) or TP53 (p53) silencing (n=3 for each cell line and condition); b. Principal component analysis (PCA) was performed on the five cell lines expression matrix. The first 3 principal components are plotted in pairs, the emerging sample groups confirmed that each cell line is a homogeneous cell population irrespective of being silenced for TP53 (triangles) or not (circles). The difference among the cell lines is larger than between the controls and the TP53 silencing; c. MDA-MB-231 cells RNA-seq samples quality control performed using FastQC. Selected results are shown. d. MDA-MB-231 cells ChIP-seq samples quality control performed using FastQC. Selected results are shown. e. Extended result from Figure 1d: transcript levels of all human 26S proteasome and immunoproteasome subunits determined in five TNBC cell lines upon mutant TP53 expression silencing using alternative siRNA – 3'UTR-targeting siRNA II (normalized control level shown as the dashed line, each result is a mean of two independent experiments). # marks a possible off-target effect of TP53 siRNA II towards PSMD10 transcript. For individual expression values of each gene in each cell line, see Supplementary Tab. 3. Statistics source data for 1e provided in Supplementary Table 10.

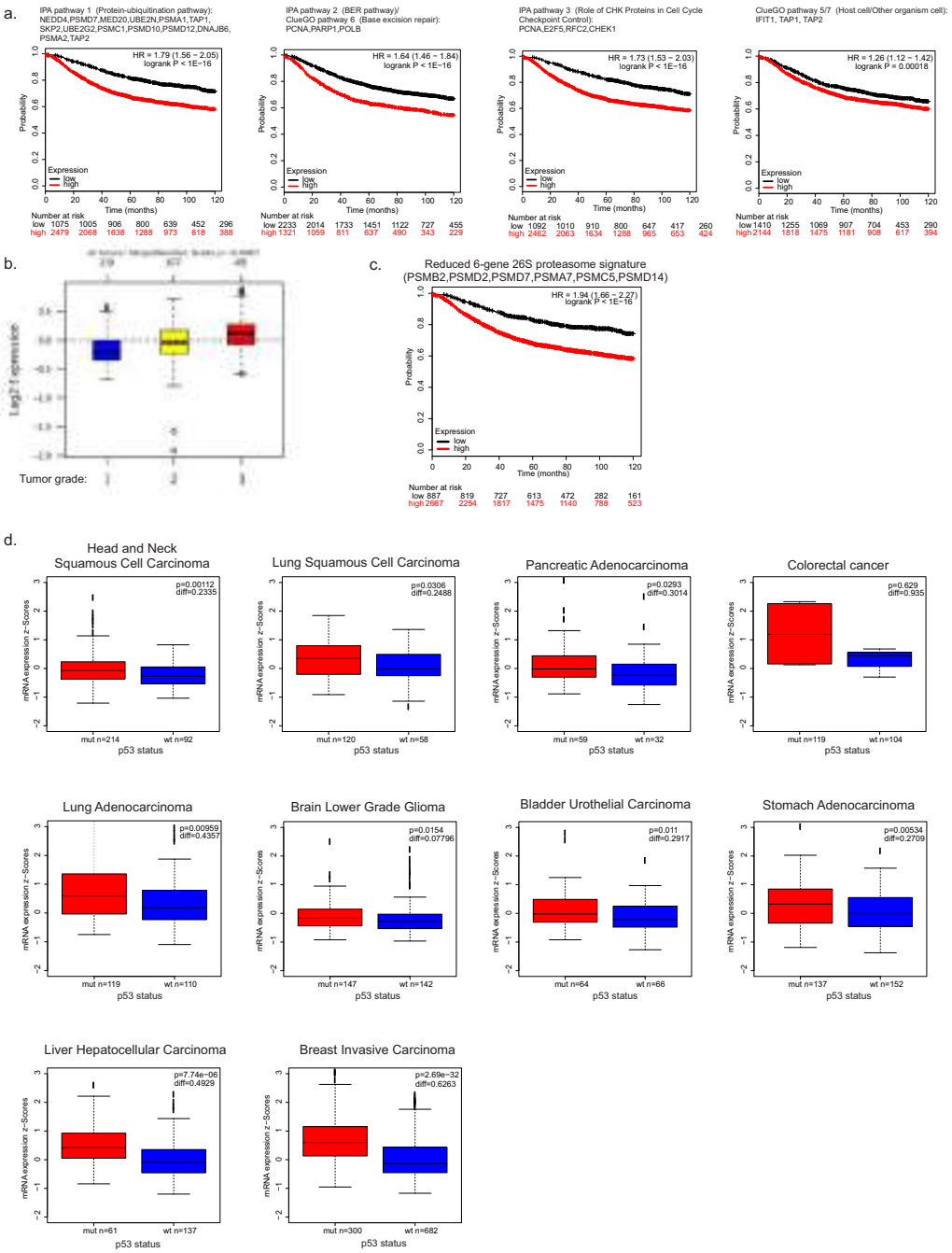

Supplementary Figure 2 a. The mutant p53-related proteasome-ubiquitination pathway gene expression is more significantly associated with poor prognosis in breast cancer patients than of the genes from other top pathways derived from the common mutant p53 signature. HR – hazard ratio; logrank P – logrank test p-value for the curves comparison (n=3458); b. The high expression of 37 proteasome genes ("whole proteasome signature") is associated with the high grade of breast cancer in patients (grades marked 1-3). P-value is derived from Mann–Whitney U test (n=1401). Box plot centre represents the median, box extremes indicate first and third quartile, whiskers extend to the extreme values included in the interval calculated as +/-1.58 IQR/sqrt(n) where IQR (interquartile range) is calculated as the third quartile minus the first quartile.; c. The best recursive feature selection analysis scoring proteasome gene subset (composed of 6 genes, see Methods and Supplementary Table 8) was evaluated for the prognostic correlation in the breast cancer dataset (survival graph as in a.; HR – hazard ratio; logrank P – logrank test p-value for the curves comparison, n=3458).; d. The high expression of 37 proteasome genes is associated with the mutant TP53 status in the indicated cancer types (diff – difference in mean signature expression in mutant vs wt p53 status samples; p-value is derived from Mann–Whitney U test). Number of patients for each cancer type is indicated below each graph, based on selection in Supplementary Table 14. Box plot centre represents the median, box extremes indicate first and third quartile, whiskers extend to the extreme values included in the interval calculated as +/-1.58 IQR/sqrt(n) where IQR (interquartile range) is calculated as the third quartile minus the first quartile.

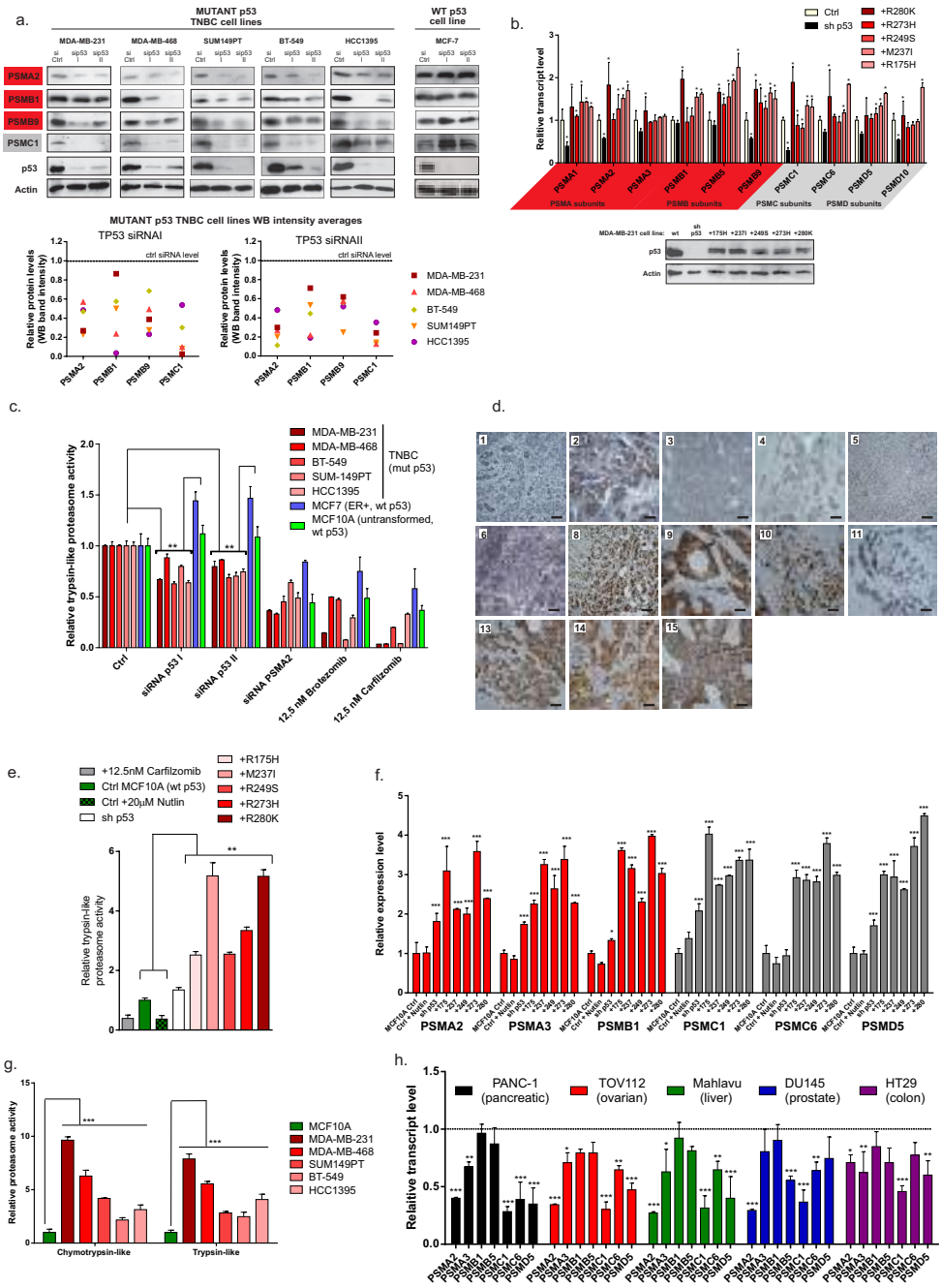

Supplementary Figure 3 a. Levels of selected proteasome subunits are lowered upon TP53 expression silencing in the 5 TNBC cell lines. Below – a bar graphs demonstrating protein levels of proteasome subunits measured by densitometry in 5 TNBC cell lines with mutant p53 (averages of two western-blots per each result are used; two alternative siRNAs – TP53 siRNA I and II; normalized control silencing level shown as the dashed line); b. Overexpressed mutant p53 variants rescue proteasome genes transcription in the stably silenced endogenous mutant TP53 background of MDA-MB-231 cells. Lower panel: western blot demonstrating stable silencing of mutant TP53 and expression of the mutant p53 variants (representative of 2 repeats); c. Trypsin-like proteasome activity is decreased in mutant p53 TNBC cell lines versus wt p53 cell lines (MCF10A and MCF7) upon silencing of mutant TP53 or PSMA2 or proteasome inhibitor treatment (24h; Carfilzomib, Bortezomib).; d. IHC staining of p53 (brown) in representative samples from Fig. 3b with indicated numbers corresponding to the Supplementary Table 15; Scale bars are 100μM; e. Trypsin-like proteasome activity in MCF10A cell lines treated with 20μM Nutlin for 24h, stably transfected with vector encoding shRNA targeting TP53 and indicated mutant p53 cds shRNA-resistant HA-tagged variants (+p53 changed residue); f. Transcript levels of proteasome subunits in MCF10A cell lines treated with 20μM Nutlin for 24h, stably transfected with vector encoding shRNA targeting TP53 and indicated mutant p53 cds shRNA-resistant HA-tagged variants (+p53 changed residue); g. Basal chymotrypsin-like and trypsin-like proteasome activities are elevated in the TNBC cell lines (mutant p53), as compared to the MCF10A cell line (wt p53).; h. Transcript levels of proteasome subunits are decreased in the indicated non-breast cancer cell lines upon mutant TP53 expression silencing. Control level is marked with the dashed line. b-c, e-h: Means of n=3 biologically independent samples with s.d. are shown, ANOVA test with Bonferroni correction: * p<0.05, ** p<0.01, *** p<0.001; Unprocessed scans of blots are shown in Supplementary Fig. 9. Statistics source data for 3a-c, e-h provided in Supplementary Table 10.

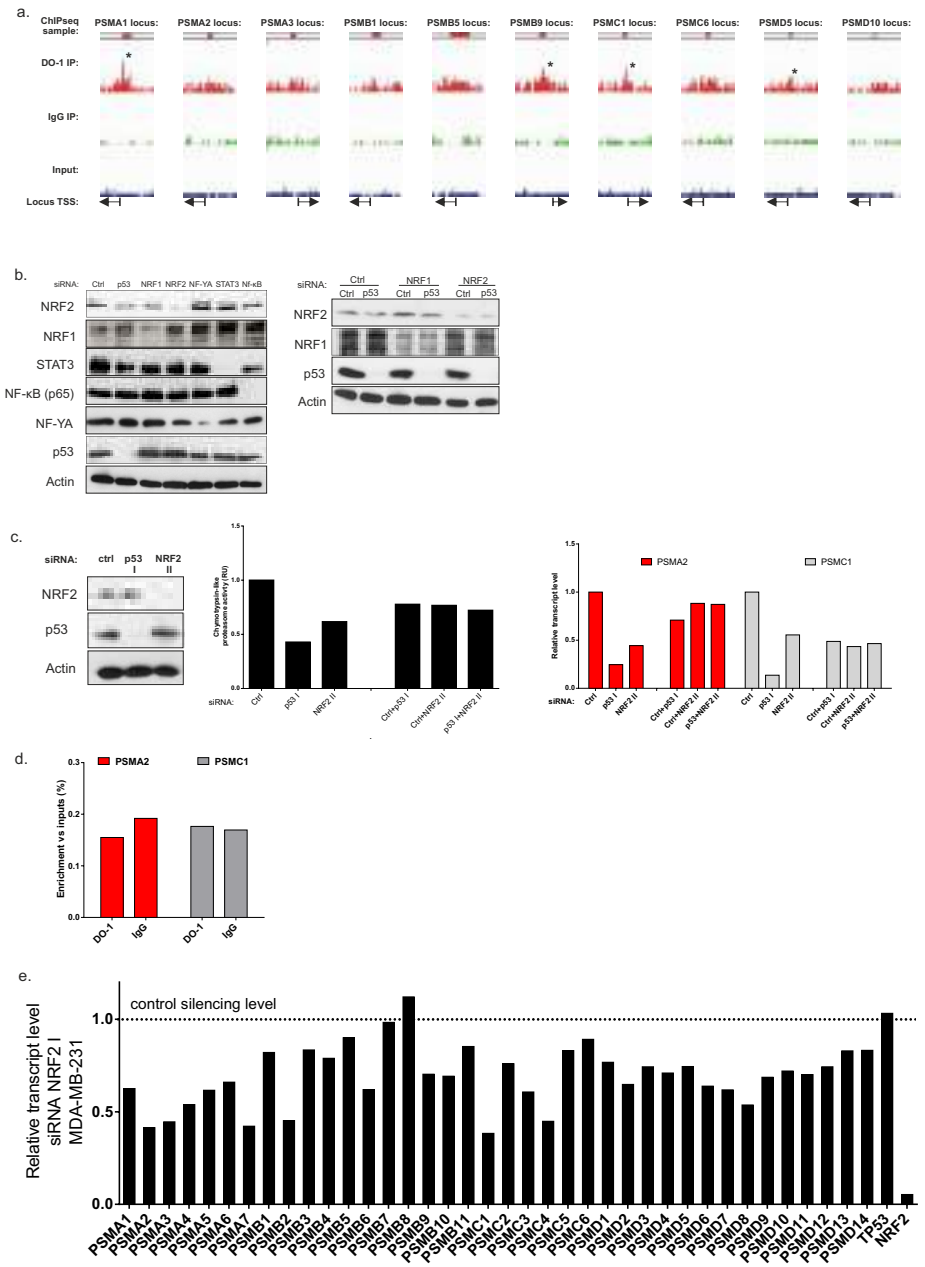

Supplementary Figure 4 a. Integrative Genomics Viewer (IGV) snapshots at the selected proteasome subunit gene loci with shown ChIP-sequencing enrichment readouts for the indicated samples in the MDA-MB-231 cells – DO-1 p53 ChIP (red), IgG ChIP (green), ChIP input (blue). (*) indicate significant peaks called in range -+500 bp of proteasome gene TSSes (Supplementary Tab. 4), other peak regions were hand-picked in IGV. Regions highlighted in red were used to design mutant p53 binding-region region primers for ChIP validation shown in Figure 4a (primers listed in the Supplementary Tab. 7); b. Western blot related to Figure 4c (left panel) and Figure 4d (right panel) showing protein levels of the transcription factors whose expression has been silenced in the indicated samples (representative of 3 repeats); c. Effects of transfection of alternative siRNA for NRF2 (NRF2 II) and siRNA for TP53 on proteasome activity (middle panel) and transcription (right panel) are comparable with siRNA NRF2 I treatment shown in Figure 4c and 4d. Means of data from two independent experiments; d. Chromatin immunoprecipitation enrichment obtained with the indicated antibodies at PSMA2 and PSMC1 mutant p53 binding regions in the wt p53 MCF7 cells – no enrichment increase is observed for DO-1 ChIP. Means of data from two independent experiments; e. Transcript levels of all human 26S proteasome and immunoproteasome subunits determined in MDA-MB-231 cells upon mutant NRF2 expression silencing (normalized control level shown as the dashed line, means of data from two independent experiments). For individual expression values of each gene see Supplementary Tab. 5. Unprocessed scans of blots are shown in Supplementary Fig. 9. Statistics source data for 4c-d provided in Supplementary Table 10.

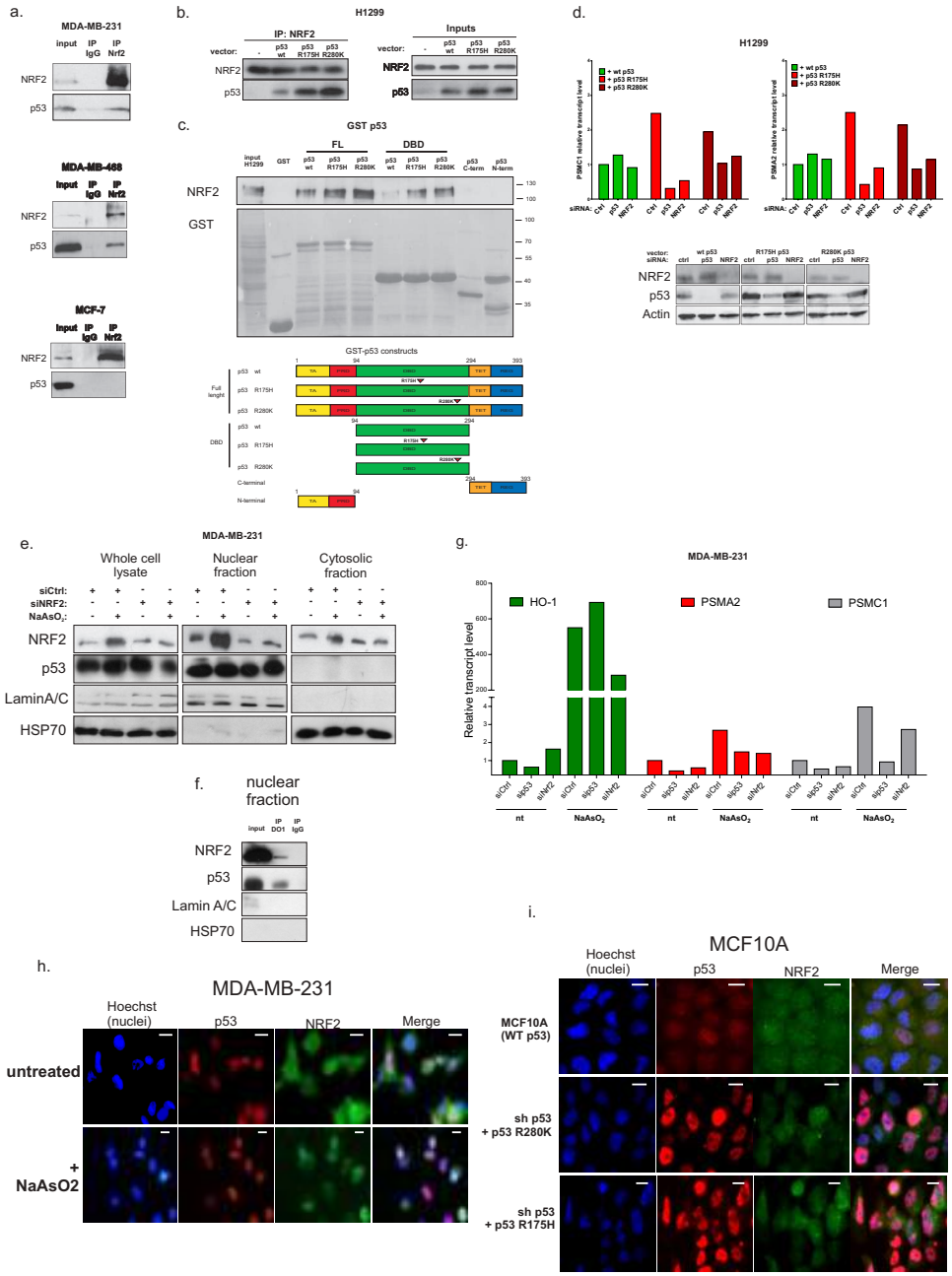

Supplementary Figure 5 a. Mutant p53 co-immunoprecipitates (co-IP) with Nrf2 in MDA-MB-231 and MDA-MB-468 cell lysates but not in MCF-7 cell lysate (anti-Nrf2 antibody). Representative of 2 repeats; b. Co-immunoprecipitation (co-IP) of Nrf2 (anti-Nrf2 antibody) and overexpressed wt or mutant (R175H and R280K) p53 in p53-null H1299 cells (representative of 2 repeats); c. GST tagged mutant p53 variants (E.coli overexpressed) interact via DNA binding domain with overexpressed full length Nrf2 in the p53-null H1299 cell lysates. (FL- full length protein; DBD – DNA binding domain; N-term – amino terminal domain; C-term – carboxy terminal domain of p53). Below a ponceau-red stained membrane is shown with transferred GST-fusion constructs (representative of 3 repeats) and a scheme of the N-terminally GST-tagged p53 constructs used for the experiment; d. The increased expression of PSMA2 and PSMC1 proteasome genes is blunted by silencing of TP53 or NRF2 in the presence of the overexpressed mutant p53 variants (R175H and R280K) in p53-null H1299 cells. The effect is absent in the wt p53 overexpressing cells (means of two independent experiments). Below – a western blot showing p53 and Nrf2 levels in H1299 upon indicated silencing (representative of 2 repeats); e. Nrf2 and p53 are present in the nuclei of MDA-MB-231 cells with or without oxidative stress. Cells optionally treated with Nrf2-targeting siRNA and/or for 6h with 50 μM of oxidative stress-inducing sodium arsenite (NaAsO2). Representative of 3 repeats; f. Mutant p53 co-immunoprecipitates with Nrf2 in the nuclear fraction of MDA-MB-231 (representative of 3 repeats); g. Mutant p53 regulates transcription of Nrf2-dependent oxidative stress induced gene HO-1 in the opposite manner to the proteasome genes. Means of two independent experiments. h. Nrf2 and p53 co-localize in the nuclei of MDA-MB-231 with or without oxidative stress. Cells optionally treated for 6h with 50 μM of oxidative stress-inducing sodium arsenite (NaAsO2). Representative of 3 repeats); i. Nrf2 and p53 co-localize in the nuclei of MCF10A control cells (wt p53) and MCF10A cells with silenced endogenous wt TP53 (sh p53) plus overexpressed mutant p53 variants (+p53 R280K. +p53 R175H). Representative of 3 repeats. Unprocessed scans of blots are shown in Supplementary Fig. 9. Statistics source data for 5d, g provided in Supplementary Table 10.

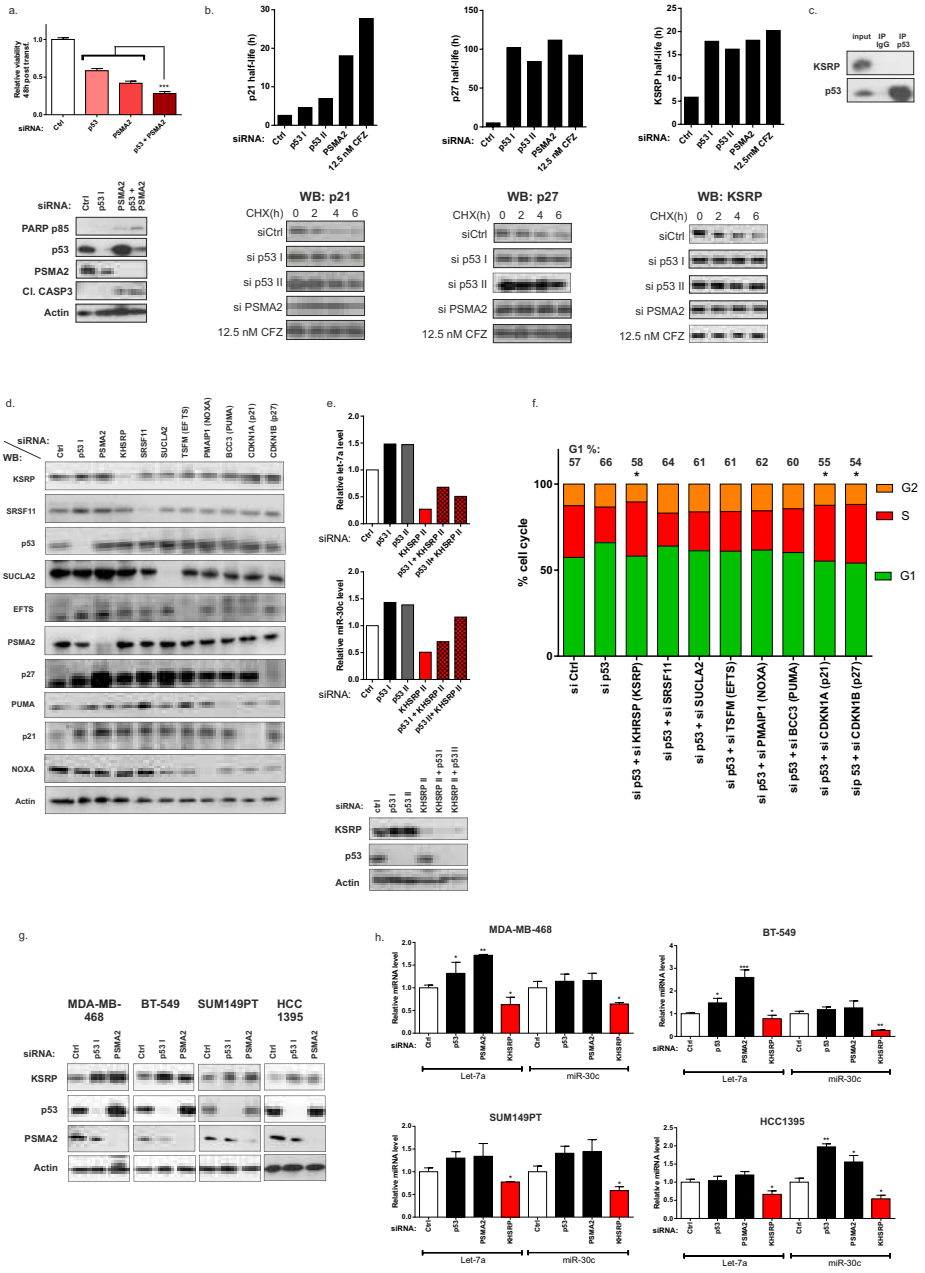

Supplementary Figure 6 a. Simultaneous silencing of mutant TP53 and essential proteasome subunit PSMA2 concomitantly decreases MDA-MB-231 cells viability and induces apoptosis markers. Bar graph represents cell viability 48 hours post silencing of mutant TP53, PSMA2 or both. Means of n=4 biologically independent samples are shown with s.d., ANOVA test with Bonferroni correction: *** p<0.001. Lower panel: western blot showing the silencing effects on p53/PSMA2 and induction of apoptosis markers: PARP p85 fragment and cleaved Caspase 3 (representative of 3 repeats).; b. Protein stability of proteasome target proteins p21, p27, KSRP is increased upon silencing of TP53, PSMA2 or treatment with the proteasome inhibitor Carfilzomib (CFZ) in MDA-MB-231 cells (half-lives and western blots are representatives of 2 repeats are shown); c. KSRP protein does not interact with mutant p53 in MDA-MB-231 cells (representative of 2 repeats); d. Protein levels of mutant p53-proteasome axis targets, upon their silencing as described in Figure 6 c-e (representative of 3 repeats); e. Effects of alternative siRNAs used for KHSRP and mutant TP53 silencing on the levels of oncosuppressive microRNAs (bar graphs). Means of two independent experiments; f. Silencing of KHSRP (KSRP), CDKN1A (p21), CDKN1B (p27) suppresses cell cycle arrest induced by mutant TP53 knockdown in MDA-MB-231 cells. Additional silencing of KHSRP (KSRP), CDKN1A (p21) or CDKN1B (p27) most efficiently restores the normal cell cycle profile (marked with *). Representative of 3 repeats; g. Mutant TP53 or PSMA2 silencing induces KSRP protein level increase in the TNBC cell lines. Representatives of 2 repeats for each cell line; h. Mutant TP53 or PSMA2 silencing induces levels of oncosuppressive microRNAs Let-7a and miR30c, while silencing of KHSRP reduces them in the indicated TNBC cell lines. Means of n=3 biologically independent samples are shown with s.d., ANOVA test with Bonferroni correction: * p<0.05, ** p<0.01, *** p<0.001; Unprocessed scans of blots are shown in Supplementary Fig. 9. Statistics source data for 6a, e, h provided in Supplementary Table 10.

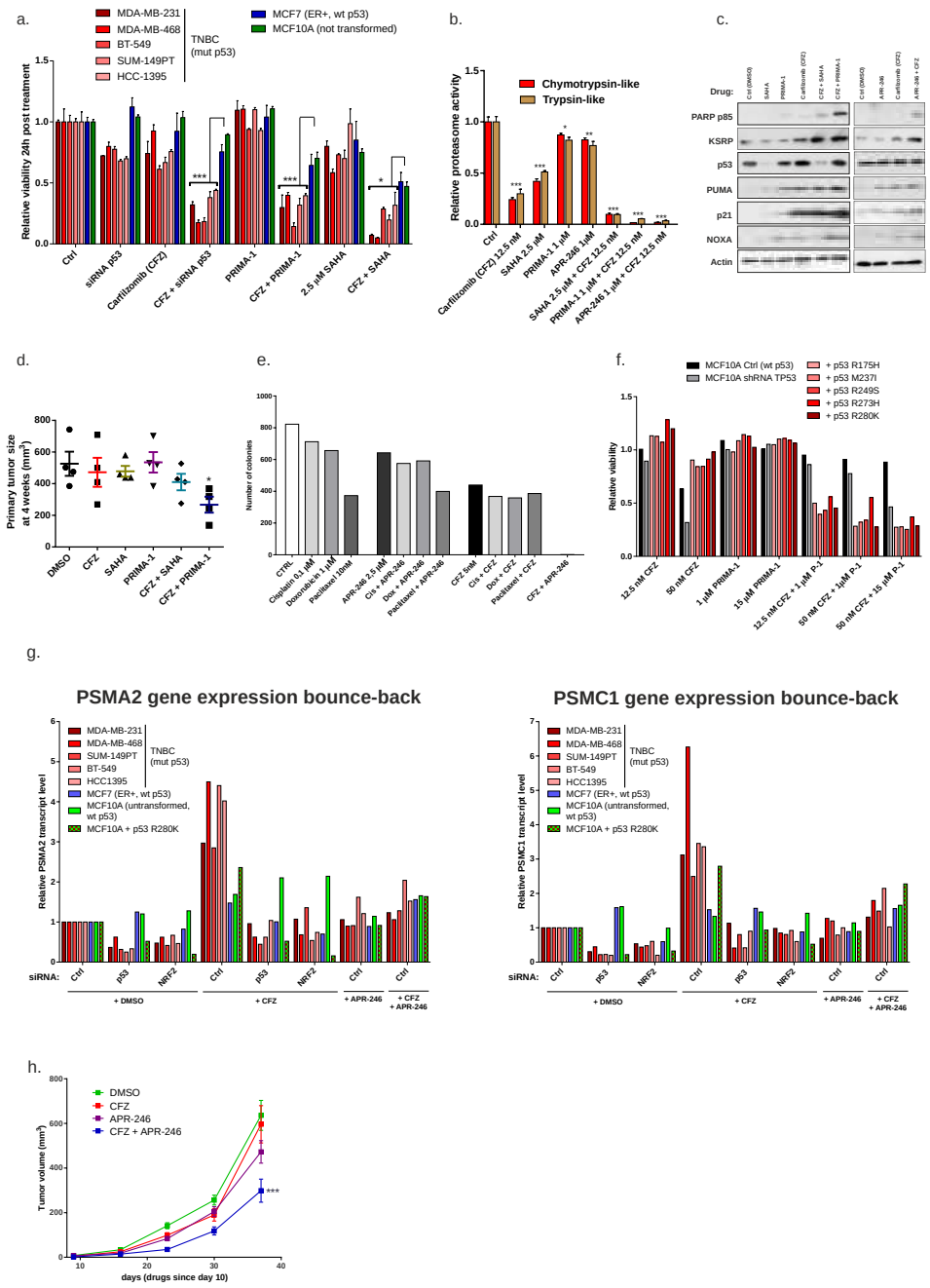

Supplementary Figure 7 a. TP53 silencing or targeting with SAHA (Vorinostat) or PRIMA-1 sensitizes TNBC but not wt p53 cell lines to the proteasome inhibitor Carfilzomib (CFZ). Viability post 24h treatment is shown. b. Drug-mediated inhibition of proteasome and mutant p53 synergistically decreases the proteasome activity in MDA-MB-231 cells. c. 24h treatment of MDA-MB-231 cells with SAHA (2,5 μM), PRIMA-1 (1 μM) or APR-246 (1 μM) plus the proteasome inhibitor Carfilzomib (CFZ; 12.5 nM) induces tumor suppressive proteins KSRP, PUMA, p21 and NOXA (latter 3 are wt p53 targets) and the apoptosis marker PARP p85 increase. Representative of 2 repeats; d. Simultaneous administration of PRIMA-1 and the proteasome inhibitor Carfilzomib (CFZ) inhibits the growth of primary xenograft tumors more effectively than a combination of SAHA and CFZ. Means of n=4 animals with s.e.m. are shown, ANOVA test with Bonferroni correction: * p<0.05, ** p<0.01, *** p<0.001; e. Concomitant treatment of MDA-MB-231 cells with Carfilzomib (CFZ) and APR-246 eliminates Carfilzomib resistant colonies while combining CFZ or APR-246 Cisplatin, Doxorubicin or Paclitaxel does not increase their toxicity. Means of two independent experiments; f. Introduction of mutant p53 variants to MCF10A cells with stably silenced wt p53 increases their resistance to proteasome inhibitor Carfilzomib (CFZ) but sensitizes them to the CFZ+APR-246 combination (viability, 24h treatment). Means of two independent experiments; g. Mutant TP53, NRF2 silencing or APR-246 (PRIMA-1MET) treatment reduces the proteasome genes PSMA2 (left graph) and PSMC1 (right graph) transcript increase due to the bounce-back effect post treatment with Carfilzomib (CFZ) in TNBC cell lines. Means of of two independent experiments; h. Primary MDA-MB-231-Luc (mutant p53, TNBC) subcutaneous xenograft growth in SCID mice is significantly reduced compared to the DMSO (caliper measurement, means of n=8 independent animals with s.e.m. are shown, significance for the time-course is indicated - Friedman nonparametric matched pairs test with Dunn's correction; *** p<0.001). a-b: Means of n=3 biologically independent samples with s.d. are shown, ANOVA test with Bonferroni correction: * p<0.05, ** p<0.01, *** p<0.001; Unprocessed scans of blots are shown in Supplementary Fig. 9. Statistics source data for 7a-b, d-g provided in Supplementary Table 10.

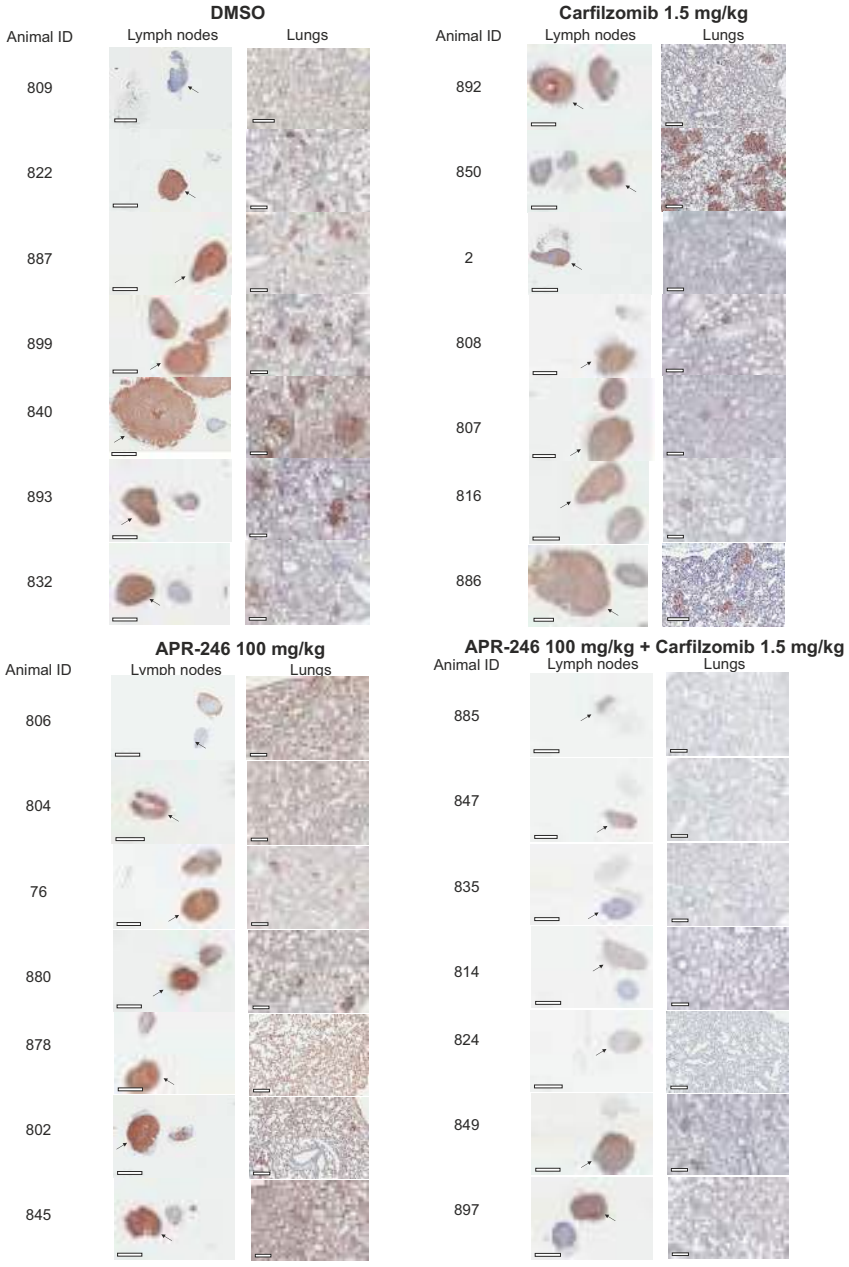

Supplementary Figure 8 Treatment of SCID mice with MDA-MB-231 cells-derived xenografts tumors using the combination of APR-246 (PRIMA-1MET) and Carfilzomib (CFZ) strongly reduces metastasis to lymph nodes and lungs. Photos of the tissue slices of lymph nodes (lymph nodes homolatreal to xenogafts - indicated by arrows; bar size – 2 mm) and lungs (bar size – 200 μm) with MDA-MB-231 metastasis IHC staining (human cytokeratin, brown) from remaining mice in the experiment shown in Figure 7g.

Fig. 3c:

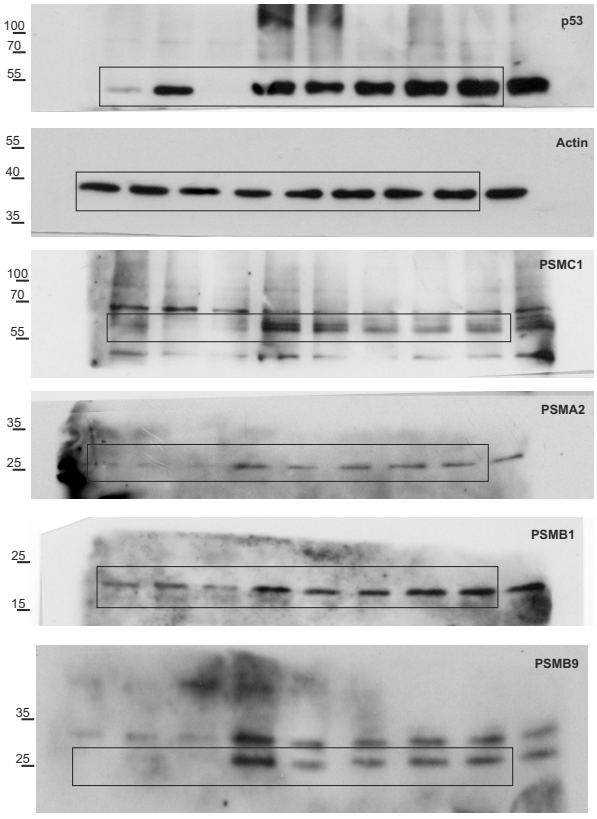

Fig. 3e:

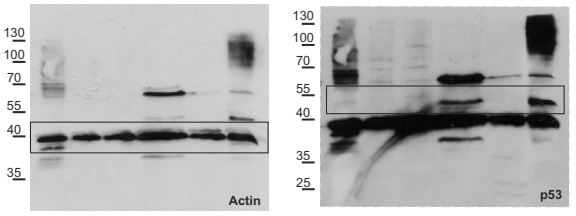

Fig. 3f:

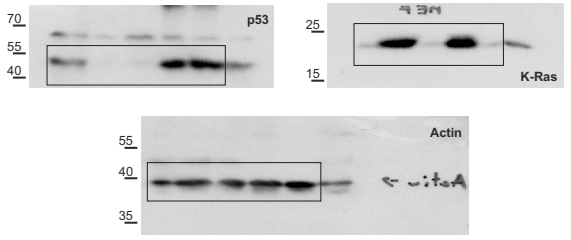

Fig. 5b:

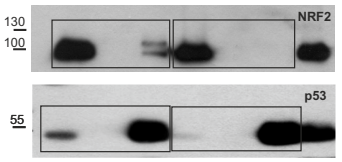

Fig. 5c:

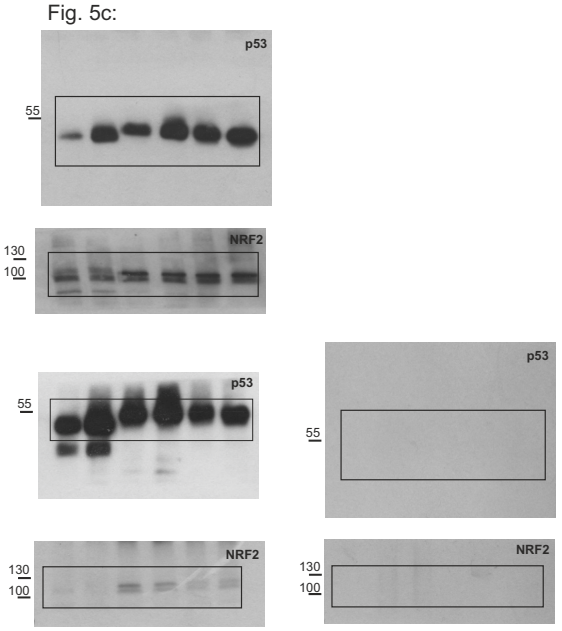

Fig. 5d:

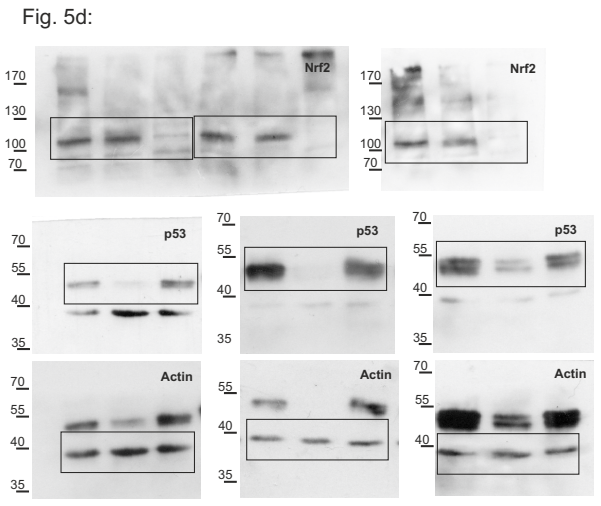

Supplementary Figure 9 Scans of developed films with approximate regions used for figures marked with rectangles and molecular sizes indicated in kDa (based on prestained protein markers).

Fig. 5a

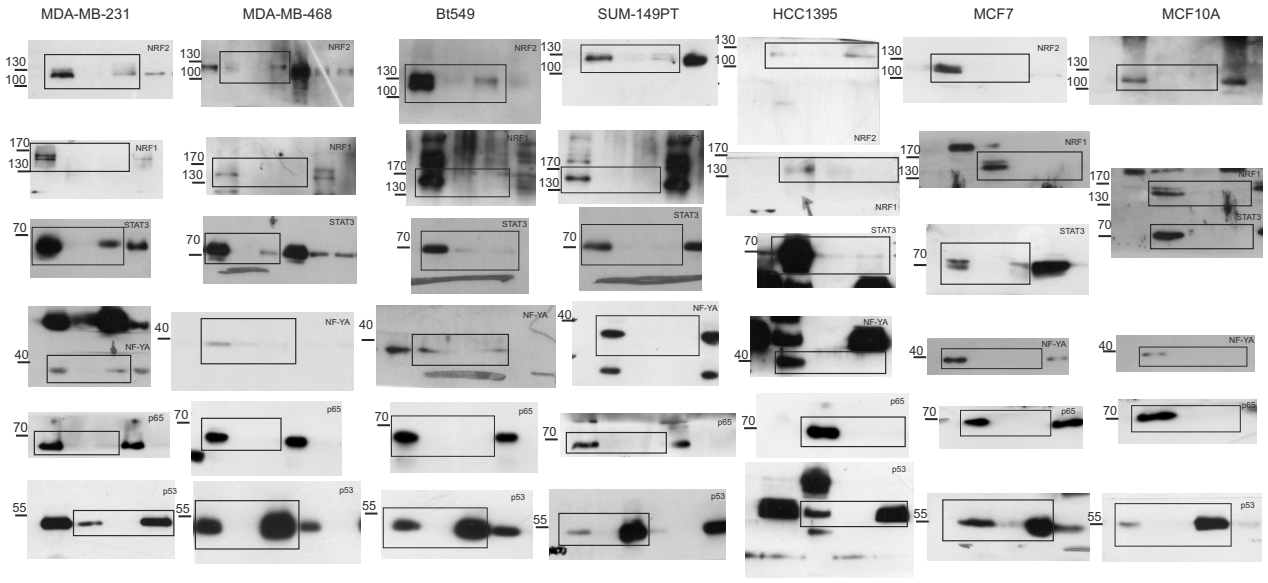

Fig. 7k:

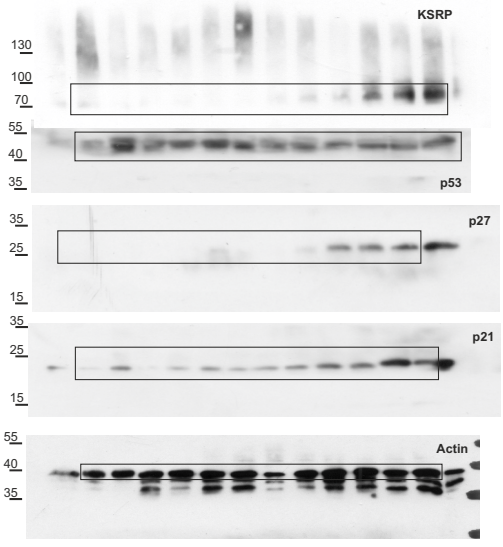

Fig. 6f:

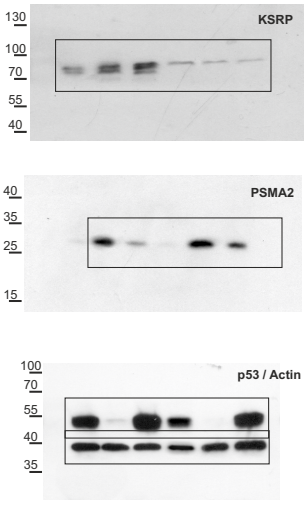

Supplementary Figure 9 continued

Supp. Fig. 3a:

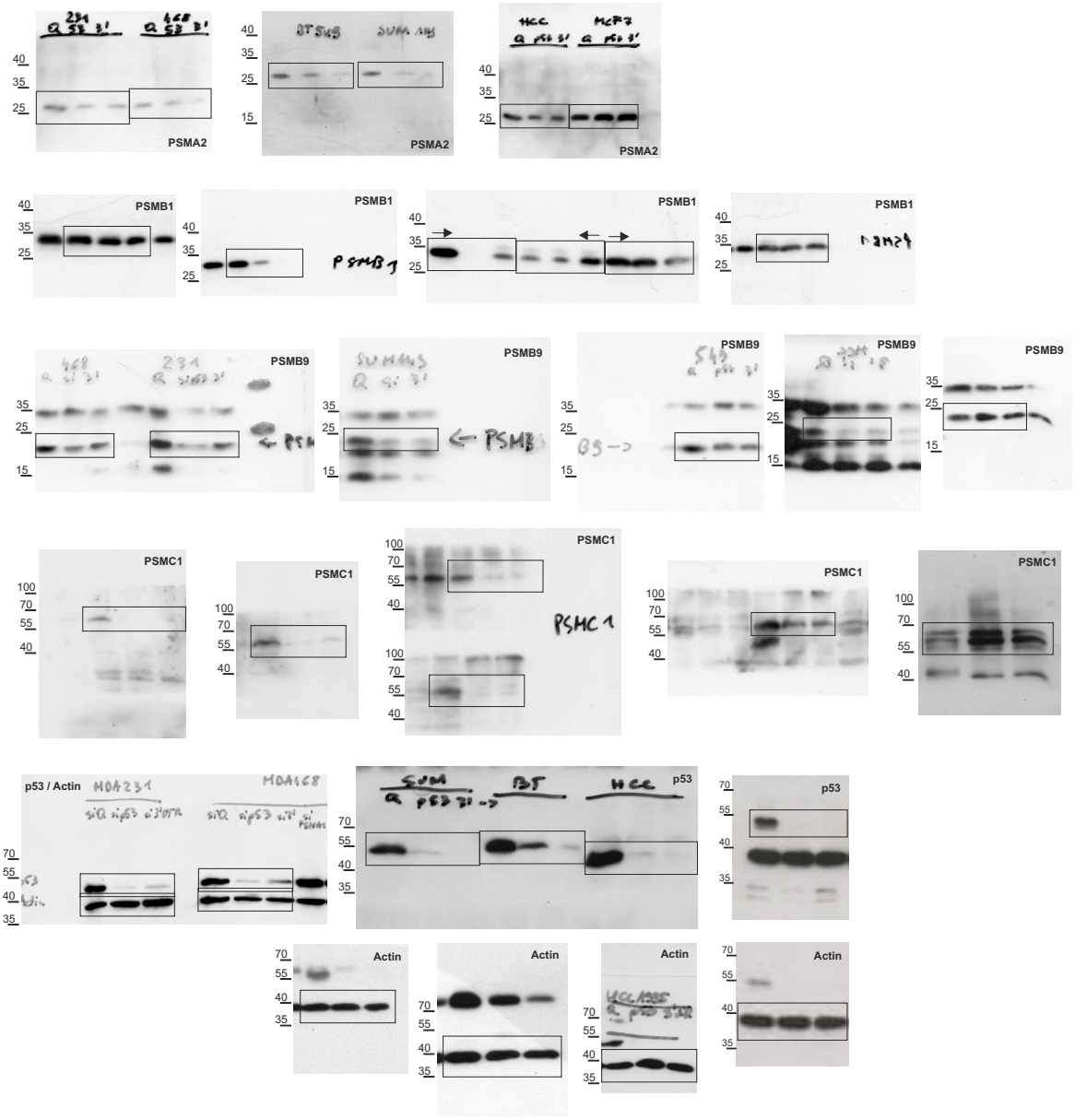

Supp. Fig. 3b:

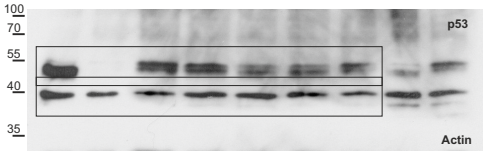

Supplementary Figure 9 continued

Supp Fig. 4b:

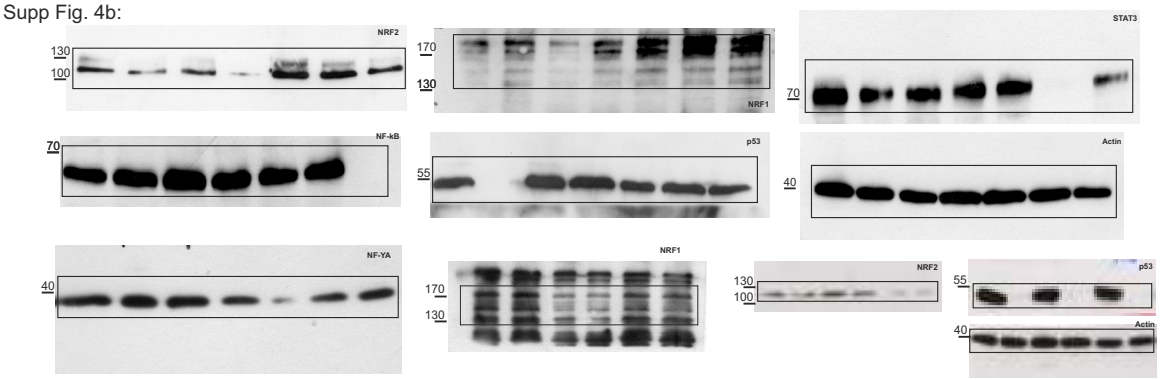

Supp Fig. 4c:

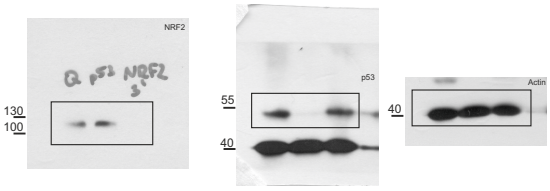

Supp Fig. 5a

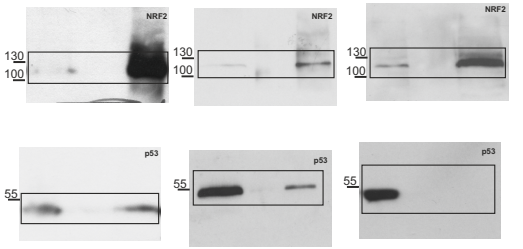

Supp Fig. 5b

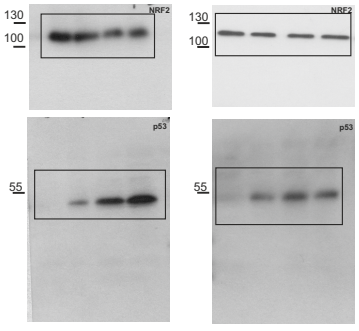

Supp Fig. 5c

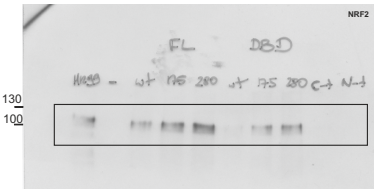

Supp Fig. 5d

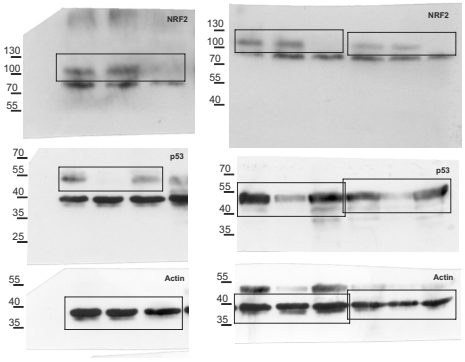

Supp Fig. 5e

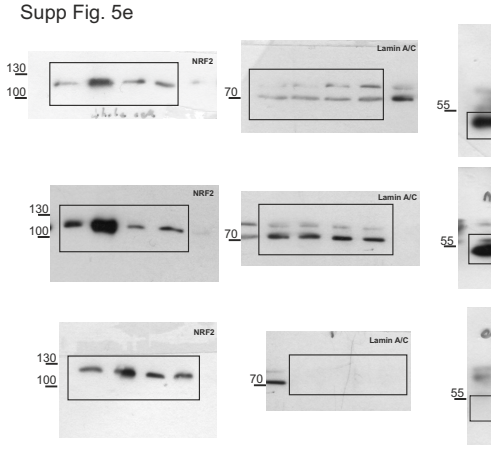

Supp Fig. 5f

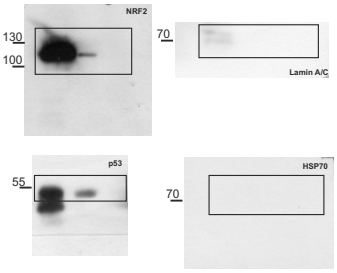

Supplementary Figure 9 continued

Supp Fig. 6a:

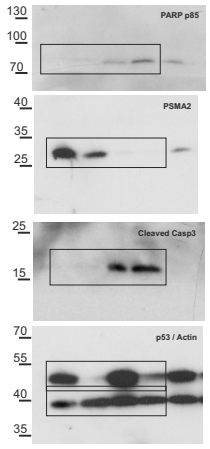

Supp Fig. 6b:

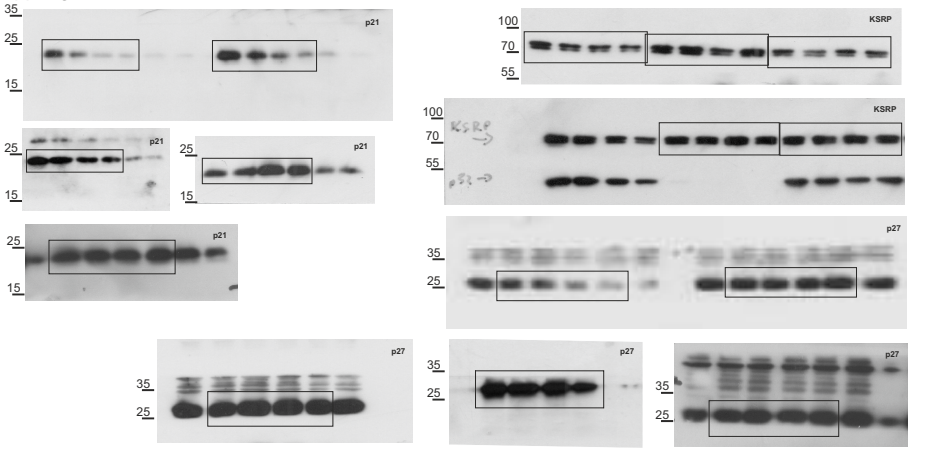

Supp Fig. 6d:

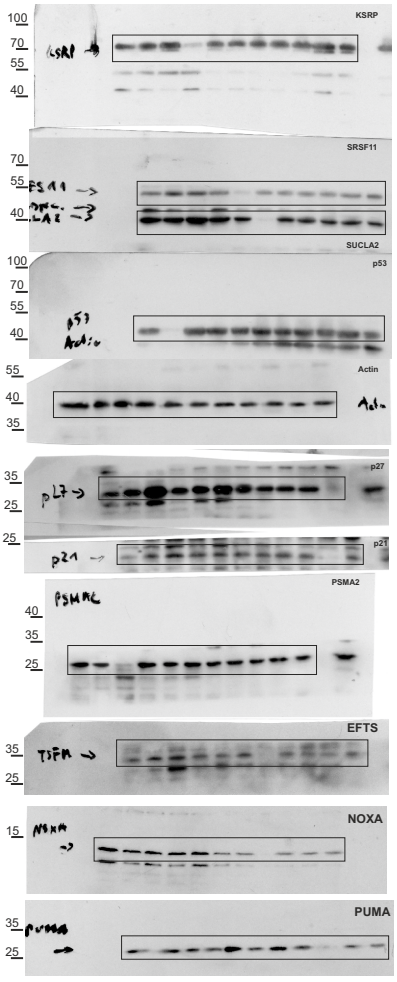

Supp Fig. 6e:

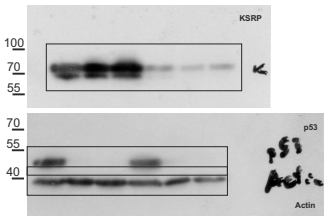

Supp fig.6c

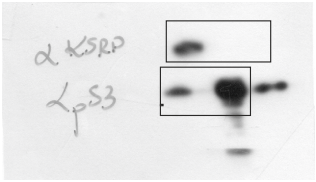

Supp Fig. 6g:

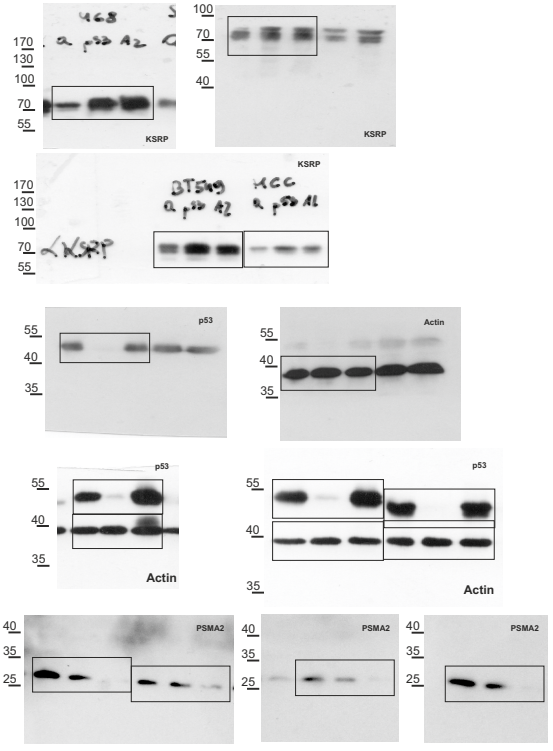

Supplementary Figure 9 continued

Supp. Fig. 7c:

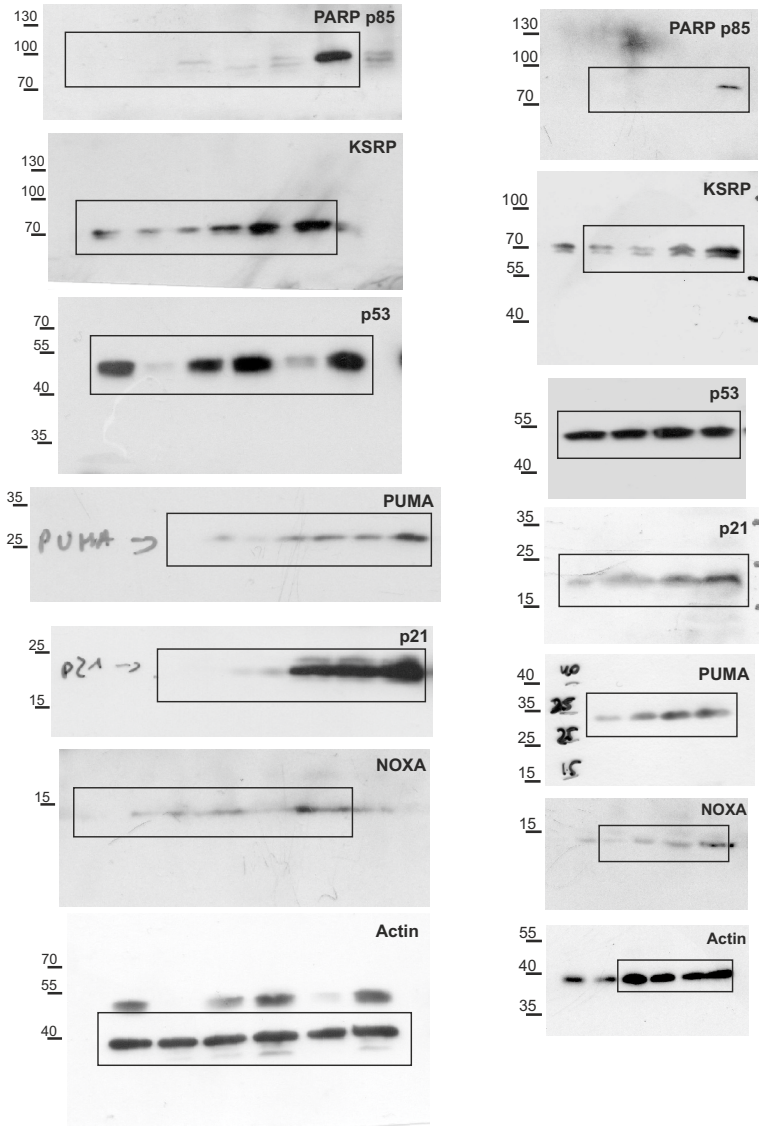

Supplementary Figure 9 continued

Supplementary Tables

Supplementary Table 1 Signatures
Gene and/or protein signatures used for pathway/GO-term, survival and gene status association analyses shown in the study. Integrated, common, mutant p53/proteasome (protein), and cell line-specific mutant p53 expression signatures are shown in worksheet tabs.

Supplementary Table 2 MDA-MB-231 Proteomic analysis
Results of total cell lysate proteomic analyses of MDA-MB-231 cells upon mutant TP53 or PSMA2 silencings (shown in worksheet tabs). Proteins identified by mass-spectrometry across all 8 samples (n=4 controls vs n=4 silencings) in both experiments are listed in the tables and used to calculate fold changes and t-test raw p-values.

Supplementary Table 3 5 TNBC Cell Lines Transcriptomics
Results of transcriptomic analyses in five indicated TNBC cell lines upon mutant TP53 silencing. Transcripts detected in all five experiments are shown (with no additional fold-change or p-value cutoffs applied): RNA-seq for MDA-MB-231 cells and Illumina HumanHT-12-v4-BeadChip for other cell lines. 37 proteasome/immunoproteasome (PSMxy) subunit genes are highlighted in blue.

Supplementary Table 4 MDA-MB-231 ChIPseq Peak Calling
Results of ChIP-sequencing peak-calling in DO-1 anti-p53 IP sample of MDA-MB-231 cells. Fold enrichements, FDRs, closest genes and their transcription start site (TSS) distances are listed for the peaks at indicated chromosome positions (tab 1). List of peaks called at -/+ 500 bp from adjacent gene TSSes (tab 2). Enrichment values for each gene/cell line included in the Fig. 4a low-scale ChIP analysis (tab 3).

Supplementary Table 5 Proteasome Transcripts qPCR
Levels of 37 proteasome/immunoproteasome transcripts in five TNBC cell lines upon silencing of mutant TP53 using two alternative siRNAs (TP53 I and II) in relation to control silencing (tab 1). Levels of 37 proteasome/immunoproteasome transcripts in MDA-MB-231 upon NRF2 silencing in relation to control silencing. Standard deviations (s.d.) are derived form n=2 (tab 2).

Supplementary Table 6 TF identification
Identification of transcription factor binding sites in mutant p53 binding regions in 37 proteasome/immunoproteasome gene promoter regions (based on ChIP-seq results form Supplementary Table 4) as descried in Methods. Transcription factors known to regulate proteasome transcription and analyzed in Fig. 4 are highlighted in yellow.

Supplementary Table 7 Primers and siRNAs
mRNA qPCR primers, ChIP qPCR primers and siRNA sequences used in the work are listed in the in worksheet tabs.

Supplementary Table 8 Feature selection analysis for proteasome signature
Full result of the feature analysis (see Methods) of the 37 genes proteasome/immunoproteasome signature shown in Supplementary Fig. 2c. The 6-gene signature with best score of association with mutant p53 status in breast cancer as well as the full 37 genes signature (with marginally worse result) are highlighted in yellow.

Supplementary Table 9 MDA-MB-231 RNAseq FPKM and Raw counts
FPKMs and Raw Counts for MDA-MB-231 RNA-seq result upon mutant TP53 silencing (n=3) vs control silencing (n=3).

Supplementary Table 10 Statistics Source Data
Data used to calculate statistics in Figs. 1d, 3a, c-f; 4a, 4d-g; 5d; 6e, h-i; 7b and Supplementary Figs. 1e, 3a-c, e-h; 4c-d; 5d,g; 6a,e,h; 7a-b, d-g.

Supplementary Table 11 Antibodies
Antibodies used in the work.

Supplementary Table 12 TNBC Cell Line Characteristics
A table characterizing the TNBC cell lines used for transcriptomic multi-cell line analysis in Figure 1b; contact – missense mutant p53 type influencing p53-promoter DNA contact, conform. - missense mutant p53 type with distorted structure of the p53 DNA-binding domain.

Supplementary Table 13 Signature Pathway Analysis
A table with gene lists and statistical support of top pathways/GO-terms enriched by IPA and ClueGO software analysis of the integrated and common signatures form Fig.1a and b (shown in separate worksheet tabs).
–log (p-value) is derived from Fisher test in IPA; –log (B-H p-value) is derived from Benjamini-Hochberg adjustment of p-values in IPA; Ratio – ratio of associated genes vs all genes in an IPA pathway;
% of As. Genes - percent represented by associated genes in a term in ClueGO; Term Pvalue – p-value of term association in ClueGO; B-H adj Pvalue - Benjamini-Hochberg adjustment of p-values in ClueGO; -log (B-H adj Pvalue) is derived from Benjamini-Hochberg adjustment of p-values in ClueGO.

Supplementary Table 14 TP53 status in TCGA datasets
TP53 status in cancer types used in analysis in Supplementary Fig. 2d. The table cells in grey were selected for analysis as the corresponding cancer types had a balanced mutant TP53 proportion (30%-70%) and number of the validated mutant TP53 samples was above 50. All datasets were derived from the TCGA repository (described in Methods).

Supplementary Table 15 TP53 status of breast cancer patients
Table listing the basal-like primary breast cancer tumor samples from patients, used to determine correlation between the p53 status and the proteasome activity (Fig. 3b). Mutations found by sequencing of the TP53 mRNA expressed in samples are indicated along with the TNBC status, immunohistochemical p53 staining intensity assessment and proteasome chymotrypsin activity measurement result (mean of 3 technical replicates each).